<conferenceacronym_correspondingauthorlastname>

Functional materials for energy, environment and biomedical applications (FARAON-2022)

Computational study on electronic and thermal stability of low energy indium oxide polytypes

Arthi Devamanoharan[a], Vasu Veerapandi[a], Ponniah Vajeeston[b*]

.

[a]*School of Physics, Madurai Kamaraj University, Madurai -625021, India*
[b]*Center for Materials Science and Nanotechnology, University of Oslo, Norway.*

Abstract

The electronic properties of the indium oxide (In_2O_3) material make it suitable for various solid-state devices such as solar cells, sensors, electrocatalysts and nanoscale transistors. Structural, electronic and thermal properties of two different polytypes of bulk In_2O_3 with low energy are studied and investigated using density functional theory (DFT). The main objective of this study is to explore the other possible stable phases of In_2O_3 and their relative stability. From structural optimization based on total energy calculations, lattice and positional parameters have been established. The electronic properties were computed by HSE-06 for the polytypes. The thermal properties including heat capacity, free energy and entropy were obtained. Observed that both polytypes have very high thermal capacity. Evaluated the mechanical stability by computing the single-crystal elastic constants. Calculated the Poisson's ratio and Bulk / Shear modulus which are above the critical value, implying that they are expected to be ductile material.

Keywords: Indium Oxide ; Stability study; DFT.

1. Introduction

Indium oxide (In_2O_3) is one of the significant transparent oxide semiconductors[1], combining optical transparency in the visible range with high conductivity approaching that of a metal. Pure In_2O_3 is hardly used in technological applications, but it is the progenitor of many transparent conducting oxides (TCO) and transparent semiconductor oxide (TOS) systems. Crystalline In_2O_3 exhibits high electron mobilities, representing its use in transparent logic elements. Metal doped In_2O_3 is drawing attention and has been widely used as transparent electrodes for flat-panel displays and solar cells. The current research on TCOs seeks superior properties of low resistivity and high mobility. Relating to the control of vacancies, electrical properties are investigated for various applications such as transparent transistors, optoelectronic devices, and spin-electronic devices[2]. The crystalline structure for many of the In_2O_3 based TCOs and TOSs is that of the Cubic (bixbyite type) structure of In_2O_3. In recent years, a notable number of papers on cubic -In_2O_3 have been published. The present work selects and studies the structural, electronic, mechanical, vibrational and thermal properties of two new In_2O_3 polytypes with low energy using density functional theory. Selected polytypes belong to a monoclinic (denoted as Mon-In_2O_3) and an orthorhombic (denoted as Ort-In_2O_3) crystal system.

2. Computational Details:

Structural, electronic and thermal properties of polytypes of low energy bulk In_2O_3 are investigated using the code of VASP[3] with the projector-augmented wave (PAW) method. To perform pseudo atomic calculations, the following electronic orbitals have been used for In and O respectively: In [$5s^2$ $5p^1$], O [$2s^2$ $2p^4$]. Periodic boundary conditions are used to determine the total energies of each cell and the trial wave functions are expanded on plane-wave basis. The *k*-point sampling within the Brillouin zone for the polytypes was carried out with 4x3x4 (Mon-In_2O_3) and 4x7x1 (Ort-In_2O_3) as special points in the Monkhorst-pack grid scheme [4]. Plane-wave basis set cut-off energy was taken as 550 eV. This ensures the satisfactory level of convergence of the energy during cell volume calculations.

*

E-mail address: ponniahv@kjemi.uio.no

From structural optimization based on total energy calculations, lattice and positional parameters have been established. Based on this, the energy volume curves were generated. The electronic properties were computed through the correlation function HSE-06[5] level. VASP is used for calculating the real space force constants of supercells and the PHONOPY[6] is used for calculating the phonon frequencies. Evaluated the mechanical stability by computing the single-crystal elastic constants and then by linear fitting of the stress-strain curve using VASPKIT. The thermal properties, including heat capacity, free energy and entropy were obtained from the calculated phonon density of states (PhDOS). Optimized crystal structures are visualized by using the tool VESTA[7]. QTGRACE –a two-dimensional graphical representation and GNUPLOT- a public domain script-driven engine is used for data visualization and curve fitting.

3. Results and discussion

3.1. Structural stability

Two different polytypes of bulk In_2O_3 are taken for structural stability studies. Selected polytypes belong to a Monoclinic (Mon-In_2O_3) and an Orthorhombic (Ort-In_2O_3) crystal system. Both Mon-In_2O_3 (mp-754531 space group $P2_1/c$) and Ort-In_2O_3 (mp-644741 space group *Pnma*) have 8 indium atoms and 12 oxygen atoms in their unit cells. Initially, a series of convergence tests including exchange-correlation potentials, cut-off energy and k-point set were conducted to get an optimized crystal structure. The calculated lattice parameters of In_2O_3 polytypes are given in Table 1.

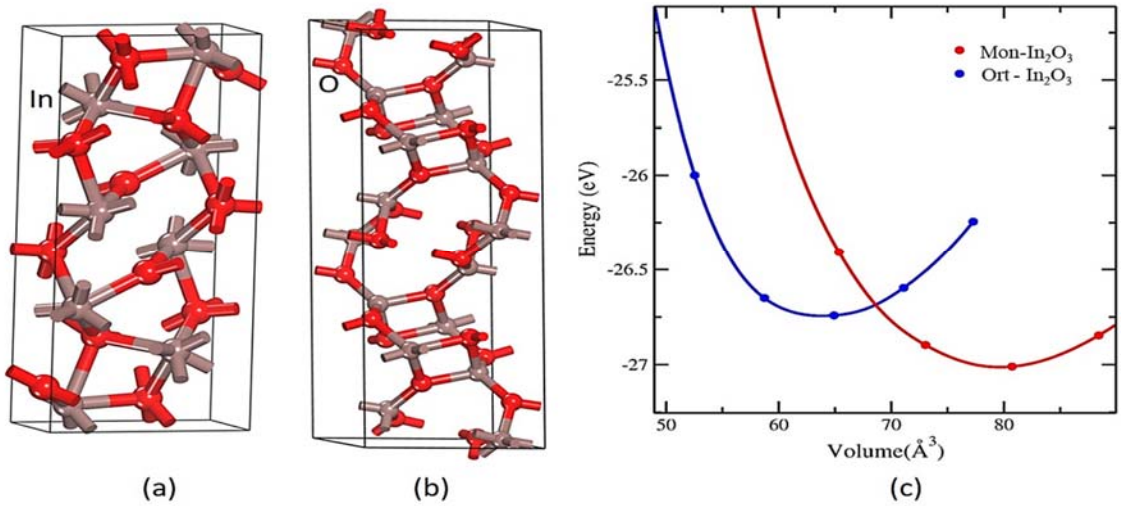

Fig. 1. The optimised structure of (a) Mon-In_2O_3 and (b) Ort-In_2O_3 ; (c) Calculated total energy(eV) as a function of unit cell volume (Å^3)

Mon-In_2O_3 polytype containing 2 types of In and three types of O atoms occupied at 4*e* sites. In the first In site, In(1) atom is bonded to five oxygen atoms to form InO_5 trigonal bipyramids. In the second In site, In(2) is bonded to four oxygen atoms to form distorted InO_4 tetrahedra. In the first and third O site, O(1) and O(3) atoms are bonded to three In atoms in a trigonal planar geometry. In the second O site, O(2) atom is bonded in a distorted trigonal non-coplanar geometry to three In atoms [Fig.1(a)]. Ort-In_2O_3 contains 2 types of In and three types of O atoms occupied at the 4*c* site [Fig.1(b)]. In the first In site, In(1) is bonded in an 8-coordinate geometry to eight O atoms. In the second In site, In(2) is bonded to seven O atoms to form distorted edge-sharing InO_7 pentagonal bipyramids. In the first O site, O(1) atom is bonded in a 5-coordinate geometry to five In atoms. In the second and third O sites, O(2) and O(3) atoms are bonded in a distorted trigonal bipyramidal geometry to five In atoms correspondingly.

For each polytype, the energy-volume curve was evaluated by allowing for full relaxation at each volume and the data were fitted to the Birch-Murnaghan equation of state [8]. Fitting the energy volume curve allows for calculating the equilibrium energy, the equilibrium volume, the equilibrium bulk modulus and its derivative.

Table 1 : Lattice parameters for the investigated In_2O_3 polytypes

Polytype Name Space Group	Unit Cell (Å)	Atom	Site	Coordinates x	 y	 z
Mon- In_2O_3	a = 6.5574 Å	In(1)	4*e*	0.95077	0.53897	0.72793
P $2_1/c$	b = 9.2746 Å	In(2)	4*e*	0.52605	0.6603	0.23208
[mp-754531]	c = 6.6691 Å	O(1)	4*e*	0.82614	0.10399	0.40561
		O(2)	4*e*	0.76359	0.01671	0.84270
		O(3)	4*e*	0.67757	0.70633	0.58861
Ort- In_2O_3	a = 5.378 Å	In(1)	4*c*	0.16475	0.25000	0.19468
Pnma	b = 2.976 Å	In(2)	4*c*	0.23555	0.75000	0.45032
[mp-644741]	c = 12.361 Å	O(1)	4*c*	0.01358	0.25000	0.39309
		O(2)	4*c*	0.13047	0.75000	0.06367
		O(3)	4*c*	0.13333	0.25000	0.77912

It is clear from Fig.1(c), that the Mon-In_2O_3 and Ort-In_2O_3 polytypes have minimum energy of -27.0 eV and -26.7 eV respectively, with an equilibrium volume of 80.7Å^3/f.u and 64.9 Å^3/f.u. The equilibrium volume for Ort-In_2O_3 is smaller, but the total energy is higher than that for Mon-In_2O_3, which indicates that Ort-In_2O_3 is less stable than Mon-In_2O_3. Further, at higher volumes and lower pressures conditions, Ort-In_2O_3 can be transformed into another phase.

3.2. Electronic structure

In-depth electronic calculations are carried out to find the viable polytype for photovoltaic cells. Our band structure calculations (HSE-06 level) states that Mon-In_2O_3 and Ort-In_2O_3 polytypes have energy gap of 1.89 eV and 2.40 eV respectively which are presented in Fig.2. The zero level of energy of the band structures is set to be at Fermi energy of respective polytypes. Valance bands of both In_2O_3 polytypes are composed of *2p* orbital of oxygen and conduction bands are resulting from *5s* orbitals of indium. The direct gap at the Gamma point is found for Mon-In_2O_3 indicates suitable for optoelectronic devices. Ort-In_2O_3 polytypes have an indirect bandgap between the symmetry points Y and Γ. The bottommost CB of Mon-In_2O_3 and Ort-In_2O_3 is dispersive and is located at the Γ point, while the topmost VB is flat, which are the important properties inherent to TCO materials[9].

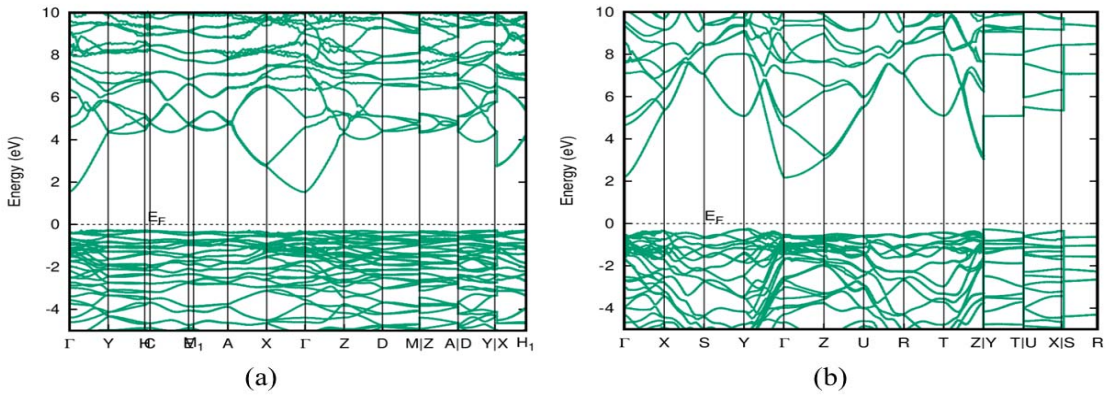

Fig. 2. Electronic band structure of (a) Mon-In_2O_3 and (b) Ort-In_2O_3 polytype

3.3. Mechanical stability

The elastic constants are used to investigate the mechanical stability of crystal systems. They are assessed by linear fitting of the stress-strain curve using VASPKIT[10]. Obtained elastic constants are operated to reproduce the various elastic parameters including Bulk, Young and Shear's moduli have been obtained by employing the Voigt-Ruess-Hill method which is shown in Table 2. Born criteria[11] of mechanical stability are obeyed by all the individual

elastic constants of both polytypes and concluded as they are mechanically stable. The bulk modulus of polytype Ort-In_2O_3 is very much higher than of Mon-In_2O_3.

An orthorhombic crystal has nine independent second-order elastic constants. For Ort-In_2O_3, it is found that C_{33} is smaller than C_{11} and C_{22} which implies that the structure is more compressible in the *c*-direction. This reflects the layered feature of the compound. The lowest value of C_{44} indicates the material's inability of resisting the shear deformation in the (100) plane. The off-diagonal shear components of the elastic constants C_{12}, C_{13}, and C_{23} are due to the resistance to volume-conserving orthorhombic distortion. Monoclinic crystal has thirteen independent second-order elastic constants. For Ort-In_2O_3, it is found that C_{22} is smaller than C_{11} and C_{33} which implies that the structure is more compressible in the b-direction.

Table. 2. The calculated single-crystal elastic constants C_{ij} (GPa), Bulk modulus B (GPa), Shear modulus G (GPa), Poisson's ratio ν, Young's modulus E (GPa) and Pugh's ratio (B/G)

Polytype Name	C_{11}	C_{12}	C_{13}	C_{15}	C_{22}	C_{23}	C_{25}	C_{33}	C_{35}	C_{44}	C_{46}	C_{55}	C_{66}	B (GPa)	G (GPa)	ν	E (GPa)	B/G
Mon-In_2O_3	111.2	18.7	43.2	-2.5	27.9	31.9	-3.3	134.4	-8.2	21.2	-8.2	26.9	21.3	38.8	22.2	0.3	56.0	1.8
Ort-In_2O_3	464.3	251.0	234.5	-	530.6	204.9	-	314.6	-	66.0	-	130.2	97.7	288.7	95.7	0.4	258.5	3.0

The bulk modulus measures the resistance to a volume change due to isotropic applied pressure and the shear modulus characterizes the resistance to plastic deformation. The Pugh's ratio (*B/G)* reflects the hardness of a material. A high (>1.75) value of the Pugh's ratio (*B*/*G*) is associated with ductility, whereas a low (< 1.75) value corresponds to brittleness. Thus, both In_2O_3 polytypes are expected to show ductile characteristics. Young's modulus (E) measures the stiffness of solid compounds and evaluates the resistance against longitudinal stress. The high value of *E* indicates that both polytypes can withstand large tensile stress. Poisson's ratio (ν) can also predict the failure mode of solids with the critical value of 0.26 [12]. The value of Poisson's ratio is 0.3 and 0.4 for Mon-In_2O_3 and Ort-In_2O_3 respectively, this implies that a metallic bonding exists in both polytypes.

3.4. Dynamical and thermal stability

Phonon calculations are done for all polytypes to understand the dynamical stability calculations. The dynamical matrices were calculated from the force constants, and phonon density of states (PhDOS) curves were computed on an 8x8x8 Monkhorst-Pack grid. The thermal properties including heat capacity, free energy and entropy, were obtained from the calculated PhDOS. Both polytypes display positive modes, which indicates that they are dynamically stable. For Ort-In_2O_3 (Fig.3) the smaller oxygen atom dominates the higher frequencies and the heavier indium atom dominates the lower frequencies. But for the Mon-In_2O_3, the contribution of both atoms spread in all frequency ranges.

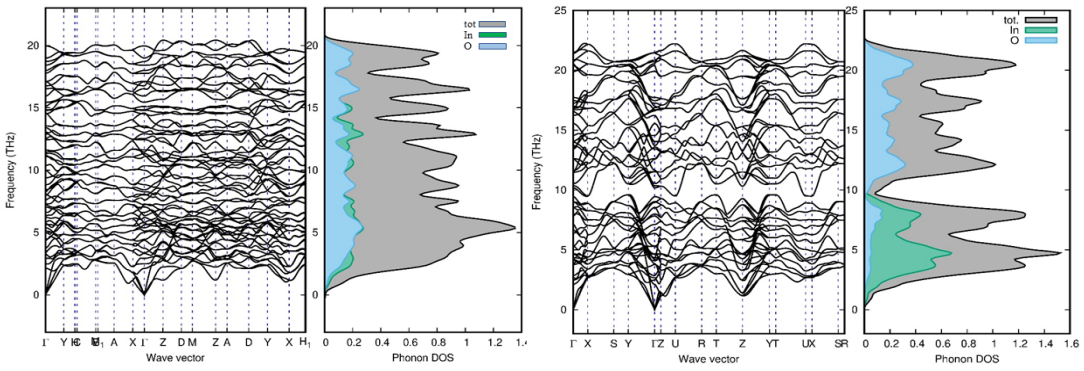

(a) (b)

Fig. 3. Phonon dispersion with Phonon density of states of (a) Mon-In_2O_3 and of (b) Ort-In_2O_3 polytypes

The symmetry of polytypes Mon-In_2O_3 and Ort-In_2O_3 can be defined by the $C_{2h}(2/m)$ and $D_{2h}(mmm)$ point groups correspondingly. Normal vibrational modes of Mon-In_2O_3 and Ort-In_2O_3 are found and they consist of 4 and 7 active modes of vibration respectively. For both polytypes, the highest active mode was found at a frequency around 5THz due to total symmetric in-plane stretching or bending movement of indium and oxygen atoms concerning the principal axis for both polytypes.

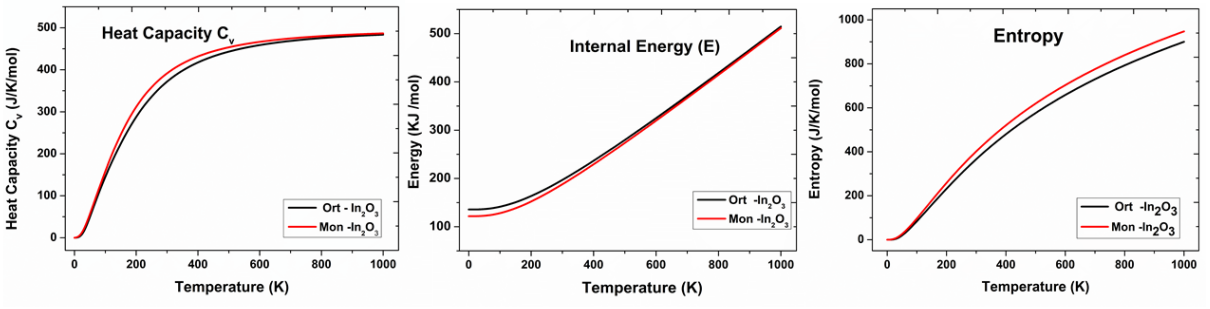

(a) (b) (c)

Fig. 4. Thermal parameters (a) Heat capacity (b) Internal energy (c) Entropy as a function of Temperature (K) for Mon-In_2O_3 and Ort-In_2O_3 polytypes

However, for Mon-In_2O_3 indium and oxygen modes appear in all frequency regions as shown in Fig.3(a). A phonon band gap between the acoustic and optical modes found in Ort-In_2O_3 indicates a high scattering-process rate and the lattice thermal conductivity is relatively low as in Fig.3(b). When the temperature of the system increases to 1000 K, Entropy increases to nearly 900 J/K/mol, internal energy reaches about 510 KJ/mol and heat capacity rises around 480 J/K/mol for both In_2O_3 polytypes which are shown in Fig. 4.

4. Conclusion

For the first time, two different In_2O_3 polytypes with space groups $P2_1/c$ and *Pnma* are proposed and studied using DFT total-energy calculations, electronic, vibrational, thermal studies and elastic constants calculations. Mon-In_2O_3 polytype has a direct bandgap of 1.89 eV and Ort-In_2O_3 polytype has an indirect bandgap of 2.4 eV. Both are dynamically as well as mechanically stable. Elastic constants are obtained and the various elastic parameters including bulk, Young and shear moduli have been calculated. From the calculated elastic parameters, concluded that both In_2O_3 polytypes are expected to be ductile materials. Ort-In_2O_3 is a stiffer polytype as its Young's modulus value is very much higher than the other. The bandgap range makes them viable for photovoltaic and photocatalytic applications. This theoretical analysis shows that the selected In_2O_3 polytypes can be readily synthesised and further experimental verification is required.

Acknowledgements

The authors acknowledge the Research Council of Norway for providing the computer time (under the project number NN2875k and NS2875k) at the Norwegian supercomputer facility.

References

[1] Edwards, P. P., Porch, A., Jones, M. O., Morgan, D. V. & Perks, R. M. Basic materials physics of transparent conducting oxides. *Dalt. Trans.* 2995–3002 (2004) DOI:10.1039/b408864f.

[2] Nagata, T. *Indium oxide: In2O3. Single Crystals of Electronic Materials: Growth and Properties* (Elsevier Ltd, 2018). DOI:10.1016/B978-0-08-102096-8.00015-X.

[3] Allouche, A. Software News and Updates Gabedit — A Graphical User Interface for Computational Chemistry Softwares. *J. Comput. Chem.* 32, 174–182 (2012). DOI: 10.1002/jcc.21057

[4] Chadi, D. J. & Cohen, M. L. Special points in the brillouin zone. *Phys. Rev. B* 8, 5747–5753 (1973). DOI: 10.1103/PhysRevB.8.5747

[5] Heyd, J., Scuseria, G. E. & Ernzerhof, M. Hybrid functionals based on a screened Coulomb potential. *J. Chem.*

Phys. 118, 8207–8215 (2003). DOI: 10.1063/1.1564060

[6] Togo, A. & Tanaka, I. First principles phonon calculations in materials science. *Scr. Mater.* 108, 1–5 (2015). DOI: 10.1016/j.scriptamat.2015.07.021

[7] Heydon, A., Levin, R., Mann, T., Yu, Y. & Ave, L. The Vesta Approach to Software Configuration Management. *Syst. Res.* (1999). web: https://jp-minerals.org/vesta/en/

[8] Katsura, T. & Tange, Y. A simple derivation of the Birch–Murnaghan equations of state (EOSs) and comparison with EOSs derived from other definitions of finite strain. *Minerals* 9, (2019). DOI: 0.3390/min9120745

[9] Karazhanov, S. Z. *et al.* Phase stability, electronic structure, and optical properties of indium oxide polytypes. *Phys. Rev. B - Condens. Matter Mater. Phys.* 76, 1–13 (2007). DOI: 10.1103/PhysRevB.76.075129

[10] Wang, V., Xu, N., Liu, J. C., Tang, G. & Geng, W. T. VASPKIT: A user-friendly interface facilitating high-throughput computing and analysis using VASP code. *Comput. Phys. Commun.* 267, (2021). DOI: 10 .17632 /v3bvcypg9v.1

[11] Mouhat, F. & Coudert, F. X. Necessary and sufficient elastic stability conditions in various crystal systems. *Phys. Rev. B - Condens. Matter Mater. Phys.* 90, 4–7 (2014). DOI: 10.1103/PhyRevB.90.224104

[12] G.N. Greaves, A.L. Greer, R.S. Lakes, T. Rouxel, Poisson's ratio and modern materials, Nat. Mater. 10 (2011) 823–837. DOI: 10.1038/nmat3134.